Brazilian Journal of Physics
ISSN: 0103-9733
luizno.bjp@gmail.com
Sociedade Brasileira de Física
Brasil

Jabbar Hussein, Mohammed; Mat Yunus, W. Mahmood; Mohamed Kamari, Halimah; Zakaria, Azmi
Thermal Diffusivity Measurement for p-Si and Ag/p-Si by Photoacoustic Technique
Brazilian Journal of Physics, vol. 45, núm. 5, 2015, pp. 518-524
Sociedade Brasileira de Física
São Paulo, Brasil

Braz J Phys (2015) 45:518–524
DOI 10.1007/s13538-015-0343-x

SOCIEDADE BRASILEIRA DE FÍSICA

GENERAL AND APPLIED PHYSICS

Thermal Diffusivity Measurement for p-Si and Ag/p-Si by Photoacoustic Technique

Mohammed Jabbar Hussein[1,2] · **W. Mahmood Mat Yunus**[1] · **Halimah Mohamed Kamari**[1] · **Azmi Zakaria**[1]

Received: 27 February 2015 / Published online: 7 August 2015

Abstract Thermal diffusivity (TD) of p-Si and Ag/p-Si samples were measured by photoacoustic technique using open photoacoustic cell (OPC). The samples were annealed by heating them at 960, 1050, 1200, and 1300 °C for 3 h in air. The thermal diffusivity of Ag-coated samples was obtained by fitting the photoacoustic experimental data to the thermally thick equation for Rosencwaig and Gersho (RG) theory. For the single layer samples, the thermal diffusivity can be obtained by fitting as well as by obtaining the critical frequency f_c. In this study, the thermal diffusivity of the p-Si samples increased with increasing the annealing temperature. The thermal diffusivity of the Ag/p-Si samples, after reaching the maximum value of about 2.73 cm^2/s at a temperature of 1200 °C, decreased due to the silver complete melt in the surface of the silicon.

Keywords Thermal diffusivity · p-type silicon · Photoacoustic technique

1 Introduction

The first demonstrations of photoacoustic (PA) and photothermal effects were made in the nineteenth century. The development of photothermal techniques started in the 1970s, particularly through the work of Rosencwaig [1, 2]. The cell acoustically isolates the microphone from external noise and contains a window enabling the modulated light to illuminate the sample [3]. The theory of the PA effect in solid sample was first described by Rosencwaig and Gersho (RG) [1]. According to this model, the heat generated in the sample will diffuse from the sample to the gas in immediate contact with the sample. An important parameter involved is the thermal diffusion length of the sample μ_s which can be defined in terms of the thermal diffusivity [4, 5],

$$\mu_s = \sqrt{\alpha/\pi f} \tag{1}$$

where f is the modulation frequency of the incident light. From the above equation, it can be seen that the μ_s decreases with the increasing modulation frequency. The modulating frequency is termed as characteristic frequency f_c (f=f_c), when the thermal diffusion length becomes equal to sample thickness l_s (μ_s=l_s), the thermal diffusivity (TD) as given by

$$\alpha_s = \pi f_c l_s^2 \tag{2}$$

TD can then be obtained by applying Eq. 2 [6, 7], which corresponds to the situation (l_s=μ_s). According to the RG theory, the rear sample periodic pressure variation in the air chamber is given by [8, 9],

$$Q = \frac{\gamma P_0 I_0 (a_g a_s)^{1/2}}{2\pi T_0 l_0 k_s f} \frac{e^{j\left(\omega t - \frac{\pi}{2}\right)}}{\sinh(l_s a_s)} \tag{3}$$

with Q given by Eq. 3. T_o, γ, and P_o are constants referring to temperature, ratio of air for heat capacities, and ambient pressure, respectively. k_s is the thermal conductivity of sample s, and the subscripts g and s represent gas and sample, respectively. Now, if the sample is thermally thin (i.e., $l_s a_s \ll 1$), Eq. 3 becomes

✉ Mohammed Jabbar Hussein
mohammed55865@yahoo.com

[1] Department of Physics, Faculty of Science, Universiti Putra Malaysia (UPM), 43400 Serdang, Malaysia

[2] Laser & Electro-Optic Centre, Directorate of Research Materials, Ministry of Science & Technology, Iraq, Baghdad, Iraq

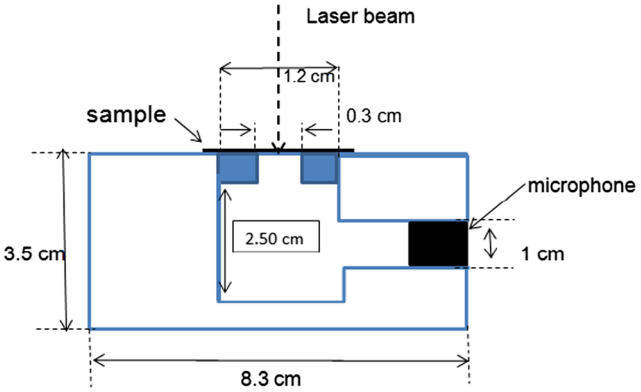

Fig. 1 Cross section of an open photoacoustic cell (*OPC*)

$$Q \cong \frac{\gamma p_0 I_0 \alpha_g^{1/2} \alpha_s}{(2\pi)^{3/2} T_0 I_g I_s k_s} \frac{e^{j\left(\omega t - \frac{3\pi}{4}\right)}}{f^{3/2}} \tag{4}$$

That is, the amplitude of the PA signal decreases as $f^{-1.5}$.

The sample is considered thermally thick (i.e., $l_s a_s \gg 1$) if the PA signal written as,

$$Q = \frac{\gamma P_0 l_o (a_g a_s)^{1/2}}{\pi T_0 l_g k_s} \frac{e^{-l_s\sqrt{\pi f/\alpha_s}}}{f} e^{j\left(\omega t - \pi/2 - l_s a_s\right)} \tag{5}$$

This equation means for the thermally thick sample the amplitude of PA signal from the rear sample decreases exponentially with modulation frequency as [3, 6, 10],

$$Q_{\text{thick}} = A/f \text{Exp}\left(-b\sqrt{f}\right) \tag{6}$$

where $b = l_s\sqrt{\frac{\pi}{a_s}}$ and l_s is the thickness of sample.

$$\alpha_s = \pi\left(\frac{l_s}{b}\right)^2 \tag{7}$$

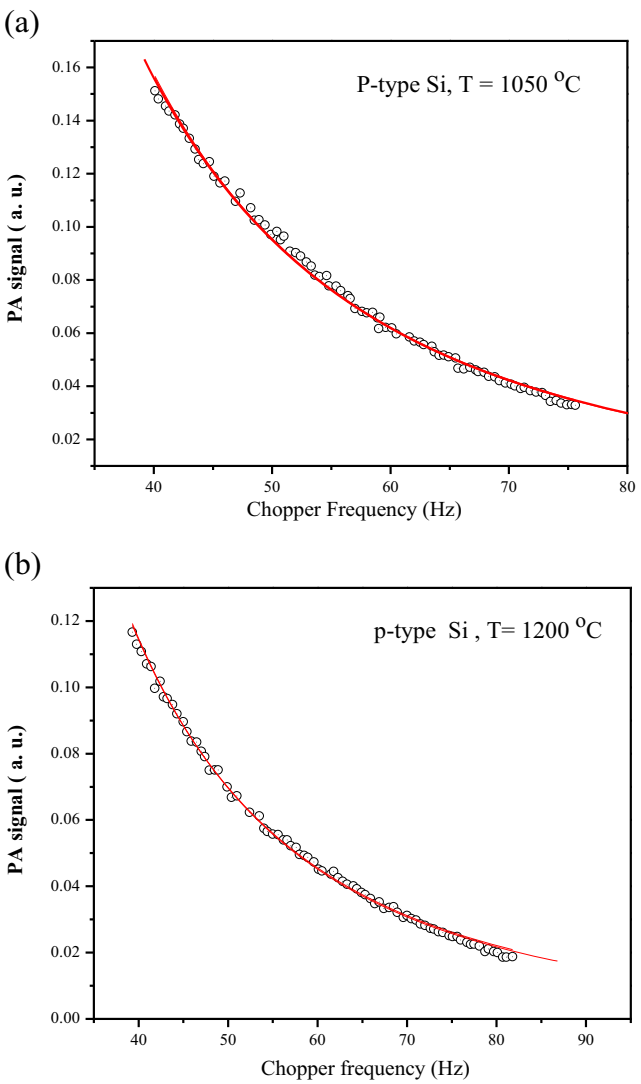

Fig. 3 PA signal vs frequency for the samples under annealing temperature **a** 1050 °C and **b** 1200 °C

TD decreased linearly with a slope of b. Hence, the TD of the sample can be easily evaluated from the signal

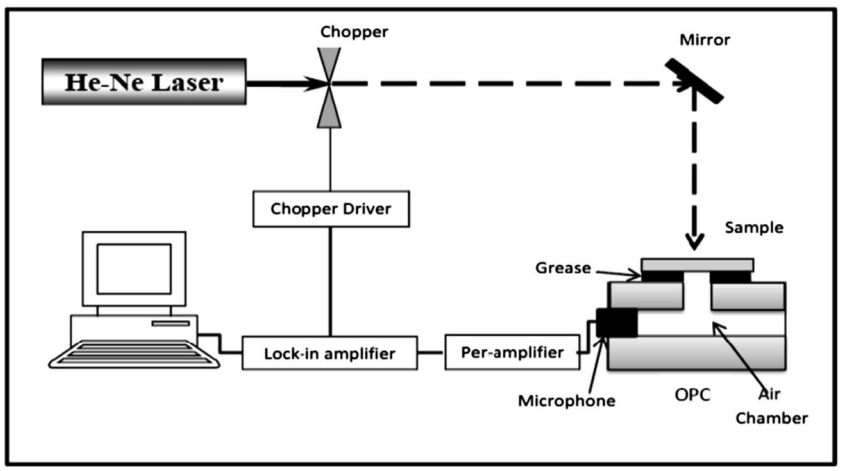

Fig. 2 Experimental set-up of the open photoacoustic cell detection technique

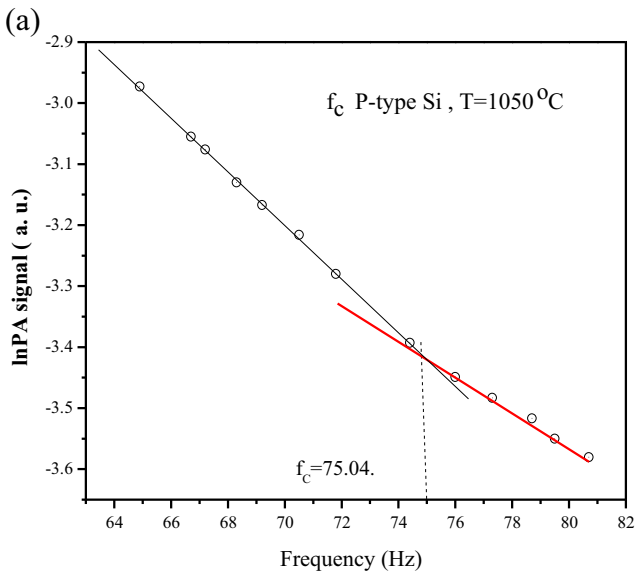

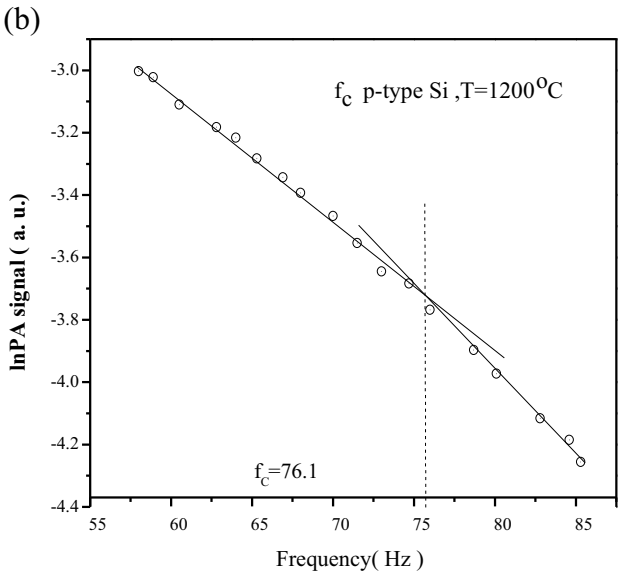

Fig. 4 Modulated frequency as function to *ln*PA signal to find f_c under annealing temperature **a** 1050 °C and **b** 1200 °C

amplitude plot. However, a necessary condition to employ the open photoacoustic cell (OPC) configuration is that the sample should be optically opaque solids at the incident wavelength ($l_\beta \ll 1$); for the thermally thick solids case ($\mu < l$, $\mu > l_\beta$), where the (μ) is thermal diffusion length, l_β absorption optical length can be obtained by $l_\beta = (1/\beta)$ and (l) the physical length. The OPC configuration can not only be used for the study of solid samples, but liquid samples can also be characterized using this configuration. Commonly used approach in the study of liquid samples using OPC configuration is by keeping the liquid in contact with a thermally thin solid sample, the thermal properties of which are known. Crystalline silicon has been widely

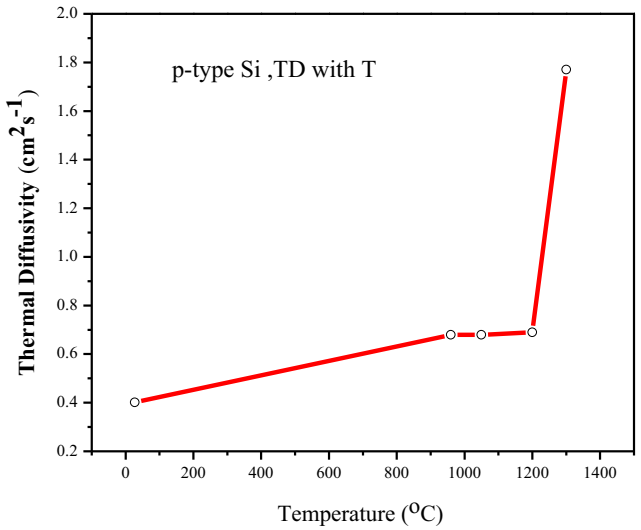

Fig. 5 Thermal diffusivity for p-type Si as a function to annealing temperature

used in optoelectronic devices [11], microelectronic devices [12], integrated circuits [13, 14], information storage, optical devices and LED diodes [15], and swells in thermoelectric composites [16]. With nanotechnology, the effect of crystallite size on the thermal properties of materials has been widely studied [17]. This material is the first choice in the industry due to its excellent semiconducting properties. The measured TD value for p-type silicon (p-Si) in room temperature wafer is 0.900–0.300 cm^2/s [18]. In this work, we used OPC to measure the TD of p-Si in annealing temperature. Silver was also added onto the silicon surface p-Si and measured the thermal diffusivity in annealing temperature.

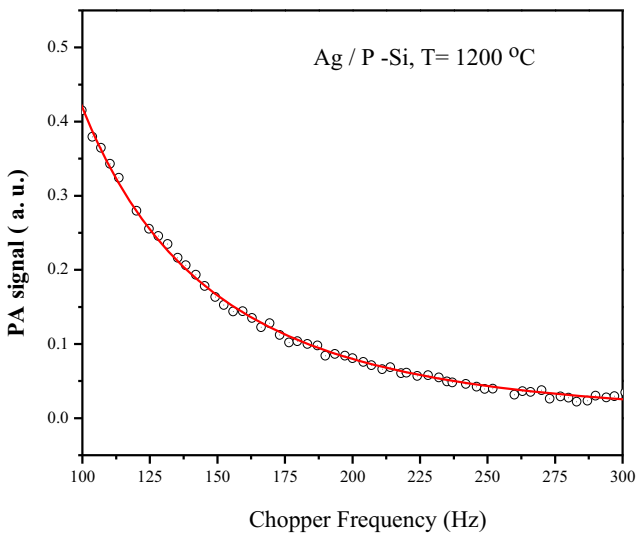

Fig. 6 PA signal versus frequency for sample 1200 °C for Ag/p-Si

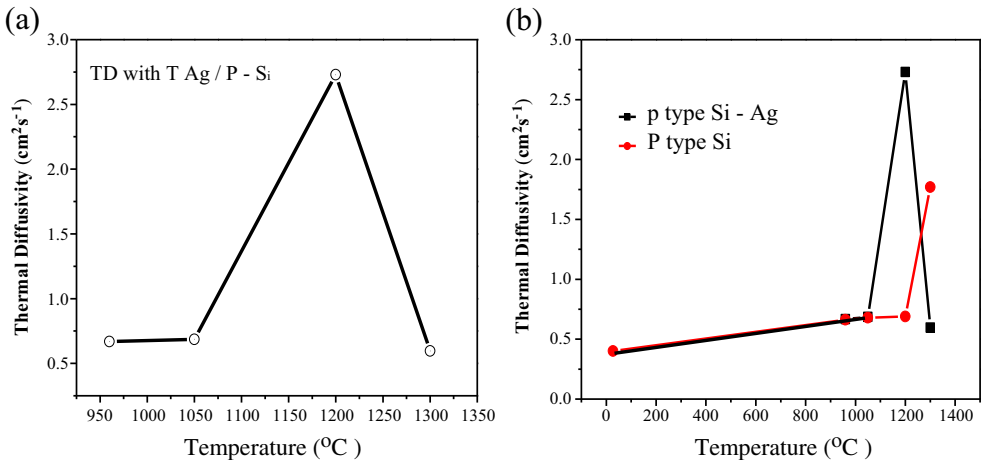

Fig. 7 Thermal diffusivity for **a** silicon with silver at different temperature, **b** comparison between p-Si and Ag /p-Si with different annealing temperature

2 Methodology

The samples used in this study are p-Si wafer which has orientation (100) and 537-μm thickness for the silicon obtained from Si Valley Microelectronics Company. The wafer was cut into a square form (2×2 cm), and to coat the silver onto it, a silver foil with a thickness of 250 μm was firmly pressed onto it. All samples were annealed by heating in air from 960 to 1300 °C. The annealing or heating time at each temperature is 3 h to diffuse the silver foil onto the silicon surface.

Figure 1 shows the cross section of an open OPC. This represents the main part of the photoacoustic spectroscopy where the cell function is to generate and detect the acoustic signal. The PA cell chamber was developed from aluminum and has an outer diameter of 8.30 cm and height of 3.50 cm. The inner cylindrical chamber is 1.20 cm in breadth, 2.50 cm in length, and 0.60 cm for the diameter of the circular opening of the cell. The cell was built with electrets microphone in the chamber as it is mounted at the second metal plate. The microphone (electrets microphone COM-08635 ROHS) acts as a pressure sensor to detect the acoustic signal.

The PA setup used continuous wave (CW) light source, He-Ne laser beam (Melles Griot, model 05LHR828) which has an output power of 75 mW, and wavelength 632 nm light source was modulated with mechanical optical chopper (SR540) from 4 to 4 kHz, Fig. 2. The signal detected by a microphone is amplified by a low noise per-amplifier (SR560) with a variable frequency bandwidth and gain that has filter ranges from 0 to 5000 kHz. The amplified photoacoustic signal (PAS) then is passed to a lock-in amplifier (SR530) to analyze and convert it into PAS amplitude and phase. The LabVIEW software was used to collect the magnitude and phase data and finally, an Origin lab 8 software was used to analyze the data.

TD for Ag-coated samples can be obtained by fitting the experimental data with Eq. 6 of thermally thick region for *b* and from it TD can be evaluated from Eq. 7 [6]. For single layer samples, the TD can be obtained by fitting as well as by obtaining the critical frequency f_c, Eq. 2. TD measurements were carried out by the PA technique using OPC technique and repeated three times to ensure the consistency of the value at room temperature. The morphological characterizations of the sample surface were carried out by using X-ray diffraction (XRD), scanning electron microscopy (SEM), and energy dispersive X-ray (EDX).

3 Results and Discussion

TD measurement of the p-type Si (p-Si) samples which has a thickness of 537 μm were measured using OPC technique cell. The chosen heating temperatures are 960, 1050, 1200, and 1300 °C, and the heating time is 3 h. The Fig. 3a, b for the PA signal amplitude of p-Si samples varies with modulation frequency under heating temperatures 1050 and 1200 °C that

Table 1 Thermal diffusivity p-Si, thermal diffusivity Ag/p-Si, and thickness for Ag/ p-Si with the different heating temperature

Anneling temperature (°C)	TD of p-Si (cm^2/s)	TD of Ag/p-Si (cm^2/s)	Thickness of Ag/p-Si (μm)
Room temperature	0.401	–	
960	0.662	0.688	720
1050	0.679	0.691	690
1200	0.689	2.730	687
1300	1.770	0.594	565

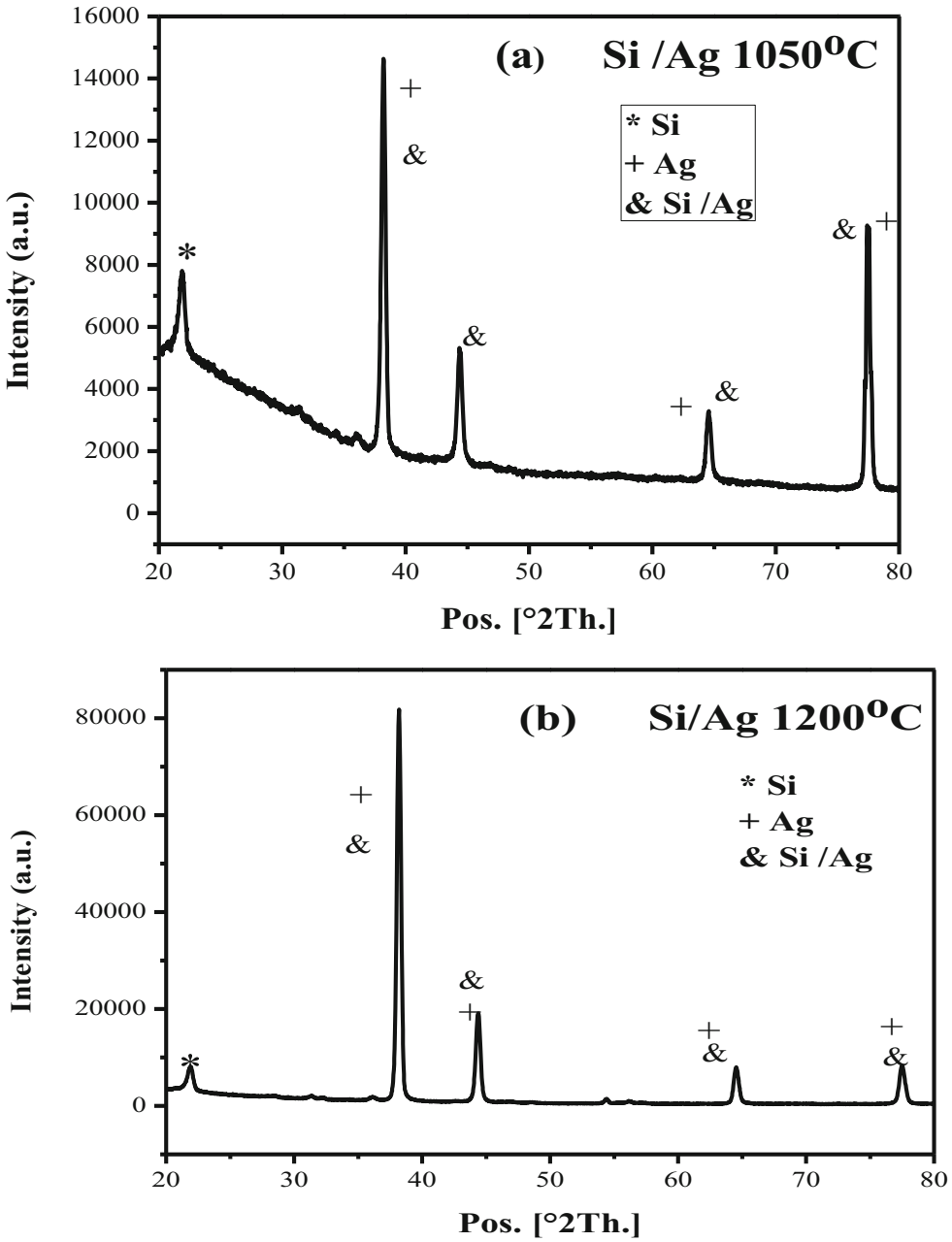

Fig. 8 *XRD* spectra for Ag/p-Si under annealing temperature **a** 1050 °C and **b** 1200 °C for 3 h

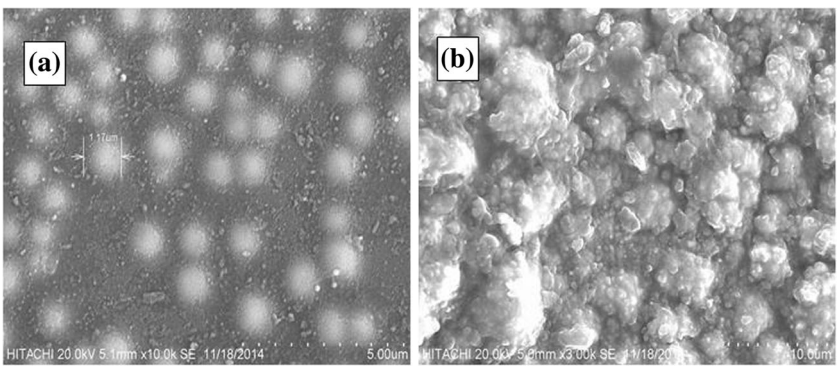

Fig. 9 SEM images for the sample under annealing temperature 1200 °C. **a** P-Si as scale 5.00 μm. **b** Ag/P-Si as scale 10.00 μm

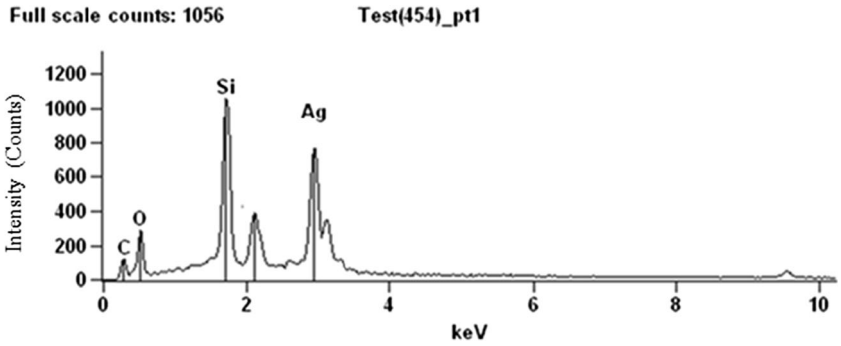

Fig. 10 EDX spectrum of the sample Ag/P-Si for the sample under annealing temperature 1200 °C for 3 h process

is clear; the PAS is decreased exponentially with increasing modulation frequency.

At room temperature, TD of unheated p-Si sample by fitting is 0.401±0.005 cm^2s^{-1}. For the heating sample at temperatures 960, 1050, 1200, and 1300 °C, the TD were 0.662± 0.005, 0.679±0.006, 0.689±0.004, and 1.770±0.005 cm^2s^{-1}, respectively.

Similar TD results can be obtained by finding f_c and using Eq. 2. For the information, the f_c of unheated sample, and samples heating at 960, 1050, 1200, and 1300 °C were 44.3, 73.1, 75.04, 76.10, and 196.06 Hz, respectively. Typical plots of *ln*(PAS) as function to modulation frequency for similar sample under heating temperatures 1050 and 1200 °C can be seen in Fig. 4.

The results show that the TD increases with annealing temperature for p-Si. Figure 5 explains the relationship between TD and temperature for p-Si with the different temperatures. Careful observation showed differences among the results of TD for p-Si due to the different temperatures used. The TD increased with increasing heating temperature for p-Si.

For the two layer Ag/p-Si sample, the typical PAS versus modulation frequency can be seen in Fig. 6 under heating up to 1200 °C. The TD is obtained by fitting experimental data with Eq. 6. For samples of heating temperatures 960, 1050, 1200, and 1300 °C in a period of 3 h, the TD were 0.688± 0.009, 0.691±0.008, 2.730±0.004, and 0.594±0.009 cm^2s^{-1}, respectively.

Figure 7a showed differences among the results of TD for Ag/p-Si due to the different temperatures used the value of TD is increased with increasing heating temperature up to heating temperature 1200 °C then decreased. The TD is decreased after complete melt of the silver. In Fig. 7b, the comparison between p-Si and Ag/p-Si could be clearly distinguished from the graph presented. The TD values of p-Si and Ag / p-Si samples are tabulated in Table 1. The melting point of pure silver is 961 °C [19]. The result show the melting point of the silver is within the range from 960 to 1200 °C (two-layer sample) [20]. The decrease of silver thickness means the silver atoms distributed through diffusion inside of the bulk of the silicon as well as evaporation of silver atoms into atmosphere. This diffusion then will limit the electron mean free path hence will lead to the decrease of TD.

The morphological characterizations of the samples surface structure were carried out by using X-ray diffraction (XRD), scanning electron microscopy (SEM), and energy dispersive X-ray (EDX).

Figure 8a, b shows the XRD analysis performed on the sample at temperatures of 1050 °C (a) and 1200 °C (b) for 3-h annealing. The peak of Si (111) and Ag (111) phase appeared at 38.09° for all silicon (Ag/p-type Si).

Figure 9 shows the image of the SEM spectrum, Fig. 9a the sample under 1200 °C the surface of silicon without silver, and the Fig. 9b the surface of silicon coated with silver under heating temperature 1200 °C after the silver complete to melt in the surface of silicon. Figure 10 EDX analyses showed strong presence for silver and has strong peak in the surface of the silicon.

4 Conclusion

In this study, the TD of the p-Si samples and Ag/p-Si samples heating at annealing temperature were successfully measured using PA technique. The results show the thermal diffusivity of the p-Si samples increased with increasing annealing temperature. However, the thermal diffusivity of the Ag/p-Si samples, after reaching the maximum value of about 2.73 cm^2/s at a temperature of 1200 °C, decreased due to the silver complete melt in the surface of silicon.

Acknowledgments The authors would like to thank the Department of Physics in the Universiti Putra Malaysia for providing the research facilities as well as Grant Putra Individu Berprestasi Tinggi of no. 9411800.

References

1. A. Rosencwaig, G. Gersho, Theory of the photoacoustuc effect with solid. J. Appl. Phys. **47**(1), 64–69 (1976)
2. A. Rosencwaig, J. Opsal, W.L. Smith, D.L. Willenborg, Detection of thermal waves through optical reflectance. Appl. Phys. Lett. **46**(11), 1013–1015 (1985)

3. J. Alexandre, F. Saboya, B.C. Marques, M.L. Ribeiro, C. Salles, M.G. Da Silva, M.S. Sthel, H. Vargas, Photoacoustic thermal characterization of kaolinite clays. Analyst **124**(8), 1209–1214 (1999)
4. G. Wang, C. Dong, Y. Shang, Y.A. Sun, D. Fu, J. Zhao, Characterization of radix rehmanniae processing procedure using FT-IR spectroscopy through nonnegative independent component analysis. Anal. Bioanal. Chem. **394**(3), 827–833 (2009)
5. P. Raji, C. Sanjeeviraja, K. Ramachandran, Thermal properties of nano crystalline CdS. Cryst. Res. Technol. **39**(7), 617–622 (2004)
6. A.M. Mansanares, A.C. Bento, H. Vargas, N.F. Leite, L.C.M. Miranda, Photoacoustic measurement of the thermal properties of two-layer systems. Phys. Rev. B **42**(7), 4477 (1990)
7. E. Marín, J.L. Pichardo, A. Cruz-Orea, P. Diaz, G. Torres-Delgado, I. Delgadillo, H. Vargas, On the thermal characterization of two-layer systems by means of the photoacoustic effect. J. Phys. D. Appl. Phys. **29**(4), 981 (1996)
8. O. Delgado-Vasallo, A.C. Valdes, E. Marin, J.A.P. Lima, M.G. Da Silva, M. Sthel, H. Vargas, S.L. Cardoso, Optical and thermal properties of liquids measured by means of an open photoacoustic cell. Meas. Sci. Technol. **11**(4), 412 (2000)
9. J.A.P. Lima, E. Marin, O. Correa, M.G. da Silva, S.L. Cardoso, C. Gatts, C.E. Rezende, H. Vargas, L.C.M. Miranda, Measurement of the thermal properties of liquids using a thermal wave interferometer. Meas. Sci. Technol. **11**(10), 1522 (2000)
10. K. Raveendranath, J. Ravi, S. Jayalekshmi, T.M.A. Rasheed, K.P.R. Nari, Thermal diffusivity measurement on LiMn2O4 and its delithiated from (MnO2) using photoacoustic technique. Mater. Sci. Eng. B **131**(1–3), 210–215 (2006)
11. C. Diaz-Guerra, A. Montone, J. Piqueras, F. Cardellini, Structural and cathodoluminescence study of mechanically milled silicon. Semicond. Sci. Technol. **17**(1), 77 (2002)
12. D.M. Gruen, Nanocrystalline diamond films 1. Annu. Rev. Mater. Sci. **29**(1), 211–259 (1999)
13. A.D. McConnell, K.E. Goodson, Thermal conduction in silicon micro- and nanostructures. Ann Rev Heat Trans. **14**(14), 129–168 (2005)
14. C.M. Poffo, J.C. de Lima, S.M. Souza, D.M. Trichês, T.A. Grandi, R.S. de Biasi, Structural, thermal and optical study of nanocrystalline silicon produced by ball milling. J. Raman Spectrosc. **41**(12), 1606–1609 (2010)
15. S. Bao, J. Yang, W. Zhu, X.A. Fan, X. Duan, J. Peng, Preparation and thermoelectric properties of La filled skutterudites by mechanical alloying and hot pressing. Mater. Lett. **60**(16), 2029–2032 (2006)
16. D.M. Trichês, S.M. Souza, C.M. Poffo, J.C. De Lima, T.A. Grandi, R.S. De Biasi, Structural instability and photoacoustic study of AlSb prepared by mechanical alloying. J. Alloys Compd. **505**(2), 762–767 (2010)
17. W.-S. Lee, T.-H. Chen, C.-F. Lin, C.-L. Wu, Microstructural evolution of nano-indented Ag/Si thin-film under different temperatures. J. Mater. Trans. **52**(10), 1868–1875 (2011)
18. K. Behzad, W.M.M. Yunus, Z.A. Talib, A. Zakaria, A. Bahrami, Effect of preparation parameters on physical, thermal and optical properties of n-type porous silicon. Int. J. Electrochem. Sci. **7**, 8266–8275 (2012)
19. A.D. Kirshenbaum, J.A. Cahill, A.V. Grosse, The density of liquid silver from its melting point to its normal boiling point 2450 K. J. Inorg. Nucl. Chem. **24**(3), 333–336 (1962)
20. S. Umekawa, R. Kotfila, O.D. Sherby, Elastic properties of a tungsten-silver composite above and below the melting point of silver. J. Mech. Phys. Solids **13**(4), 22 (1965)